*Int. J. Exp. Path.* (2008), 89, 264–275
doi: 10.1111/j.1365-2613.2008.00588.x

ORIGINAL ARTICLE

# Increased pancreatic islet mass is accompanied by activation of the insulin receptor substrate-2/serine-threonine kinase pathway and augmented cyclin $D_2$ protein levels in insulin-resistant rats

Alex Rafacho*, Daniele Lisboa Ribeiro†, Antonio Carlos Boschero*, Sebastião Roberto Taboga‡,[1] and José Roberto Bosqueiro§,[1]

*Department of Physiology and Biophysics, Institute of Biology, State University of Campinas (UNICAMP), São Paulo, Brazil, †Department of Cell Biology, Institute of Biology, State University of Campinas (UNICAMP), São Paulo, Brazil, ‡Department of Biology, Institute of Biosciences, Humanities and Exact Sciences, São Paulo State University (UNESP), São Paulo, Brazil and §Department of Physical Education, Faculty of Sciences, São Paulo State University (UNESP), São Paulo, Brazil

INTERNATIONAL JOURNAL OF EXPERIMENTAL PATHOLOGY

Received for publication:
29 January 2008
Accepted for publication:
3 March 2008

**Correspondence:**
Alex Rafacho
Departamento de Fisiologia e Biofísica
CP 6109
IB, UNICAMP
Rua Monteiro Lobato, s/n
Cidade Universitária
Campinas
São Paulo
Brazil 13083-970
Tel.: +55 19 35216198
Fax: +55 19 35216185
E-mail: rafacho@unicamp.br

[1]These authors contributed equally to this work.

## Summary

It is well known that glucocorticoids induce peripheral insulin resistance in rodents and humans. Here, we investigated the structural and ultrastructural modifications, as well as the proteins involved in beta-cell function and proliferation, in islets from insulin-resistant rats. Adult male Wistar rats were made insulin resistant by daily administration of dexamethasone (DEX; 1mg/kg, i.p.) for five consecutive days, whilst control (CTL) rats received saline alone. Structure analyses showed a marked hypertrophy of DEX islets with an increase of 1.7-fold in islet mass and of 1.6-fold in islet density compared with CTL islets ($P < 0.05$). Ultrastructural evaluation of islets revealed an increased amount of secreting organelles, such as endoplasmic reticulum and Golgi apparatus in DEX islets. Mitotic figures were observed in DEX islets at structural and ultrastructural levels. Beta-cell proliferation, evaluated at the immunohistochemical level using anti-PCNA (proliferating cell nuclear antigen), showed an increase in pancreatic beta-cell proliferation of 6.4-fold in DEX islets compared with CTL islets ($P < 0.0001$). Increases in insulin receptor substrate-2 (IRS-2), phosphorylated-serine-threonine kinase AKT (p-AKT), cyclin $D_2$ and a decrease in retinoblastoma protein (pRb) levels were observed in DEX islets compared with CTL islets ($P < 0.05$). Therefore, during the development of insulin resistance, the endocrine pancreas adapts itself increasing beta-cell mass and proliferation, resulting in an amelioration of the functions. The potential mechanisms that underlie these events involve the activation of the IRS-2/AKT pathway and activation of the cell cycle, mediated by cyclin $D_2$. These adaptations permit the maintenance of glycaemia at near-physiological ranges.

**Keywords**
cell cycle proteins, glucocorticoid, insulin resistance, pancreatic islet, structure, ultrastructure

Insulin resistance is associated with the pathogenesis of *diabetes mellitus*, which constitutes one of the main threats to human health (Anderson *et al.* 2003). The knowledge of the morphological and functional mechanisms that accompany insulin resistance is important, as this may aid in the development of future preventive therapies. The capacity of dexamethasone (DEX) to induce peripheral insulin resistance *in vivo* (Saad *et al.* 1993; Barbera *et al.* 2001; Severino *et al.* 2002; Nicod *et al.* 2003) and *in vitro* (Burén *et al.* 2002; Ruzzin *et al.* 2005) has been previously demonstrated and, depending on the dose and time of treatment, can cause type 2 diabetes (Pagano *et al.* 1983; Beard *et al.* 1984; Hoogwerf & Danese 1999). During the insulin resistance state, alterations are observed in the glucose metabolism in peripheral tissues such as liver, muscle and adipose tissues (as a result of the failure of these tissues to respond to insulin). These alterations were accompanied by functional and morphological changes in pancreatic beta cells. Peripheral insulin resistance provokes increased plasma insulin levels as a consequence of oversecretion of insulin by pancreatic islets in an attempt to keep the glycaemia close to physiological ranges (Barbera *et al.* 2001; Severino *et al.* 2002; Nicod *et al.* 2003). Insulin resistance also induces an increase in total pancreatic insulin content (Bonner-Weir *et al.* 1981) and a higher glucose-stimulated insulin secretion (GSIS) by islets *ex vivo* (Novelli *et al.* 1999; Holness *et al.* 2005). Compensatory islet hypertrophy towards chronic glucocorticoid treatment *in vivo* (Visser *et al.* 1979; Tomita *et al.* 1984; Zwicker & Eyster 1993) and in animal models that exhibit insulin resistance (Ogawa *et al.* 1992; Pick *et al.* 1998) has been described as the main morphological adaptation in this condition. The pancreatic beta-cell mass results from a dynamic balance of neogenesis, proliferation, cell volume changes and cell death (Bonner-Weir 2000, 2001). However, the molecular mechanisms involved in the regulation of beta-cell mass are not yet completely elucidated. Increased expression or activity of proteins related to the islet function and to the control of $G_1$/S cell cycle progression, such as insulin receptor substrate-2 (IRS-2), serine-threonine kinase AKT, cyclin $D_1$, cyclin $D_2$, cyclin-dependent-kinase-4 (CDK4) and p21 have been associated with augmented islet mass (Cozar-Castellano *et al.* 2004; Zhang *et al.* 2005; Fatrai *et al.* 2006; Niessen 2006; Fernández *et al.* 2006; Terauchi *et al.* 2007).

Recently, using different doses of DEX administration *in vivo*, it was demonstrated that the dose of 1.0 mg/kg induces marked peripheral insulin resistance and decreased glucose tolerance (Rafacho *et al.* 2008). Islets from these animals exhibited adaptive compensations, including increases in glucose- and other secretagogue-induced insulin secretion. The structural and ultrastructural data on pancreatic islets, referring to glucocorticoid-induced insulin resistance, are scarce; however, the majority of these studies only demonstrate islet hypertrophy as a compensatory adaptation to peripheral insulin resistance (Boquist 1972; Jonas *et al.* 1983; Tomita *et al.* 1984). Unfortunately, other studies employing prolonged periods of treatment with glucocorticoids refer to pancreatic islet observations in relation to diabetic conditions (Visser *et al.* 1979; Diani *et al.* 1987; Zwicker & Eyster 1993; Momose *et al.* 2006). Thus, the current study sought to investigate the structure and ultrastructure of pancreatic rat islets, as well as some target proteins involved in the function and control of beta-cell cycle progression in insulin-resistant rats.

## Materials and methods

### *Animals*

Experiments with animals were approved by the institutional (UNESP) Committee for Ethics in Animal Experimentation and conform to the *Guide for the Care and Use of Laboratory Animals* published by the US National Institutes of Health (NIH publication no. 85-23, revised 1996). Groups of five male Wistar rats (3 months old) from the breeding colony at UNESP were kept at 24 °C on a 12h light/dark cycle. The rats had free access to food and water. DEX-treated rats received daily injections of DEX (1mg/kg b.w., i.p., Decadron®; Aché, Campinas, Brazil) for 5 days, whereas control (CTL) rats received saline. On the day following the last DEX administration, fed rats were killed by exposure to $CO_2$, followed by decapitation. The blood was collected and immediately centrifuged. The serum insulin levels were detected by radioimmunoassay (RIA), utilizing guinea-pig anti-rat insulin antibody and rat insulin as standard (Scott *et al.* 1981).

### *Intraperitoneal insulin tolerance test (ipITT)*

The ipITT was performed in separate groups as described in detail previously (Rafacho *et al.* 2007, 2008).

### *Structural and quantitative approaches*

To study the morphological aspects and islet mass of endocrine pancreas, five pancreases from each group were excised, cleared of fat and lymph nodes, weighed, immersion-fixed for 12 h in Bouin's fixative solution, dehydrated and embedded in paraffin. At 250 μm intervals, four serial sections (5 μm) were cut on a rotary microtome and adhered to individual normal or silanized glass. The first section from each series

 

was stained with Gömori's trichrome to perform the morphological and stereological analysis. The second, third and fourth sections were immunoperoxidase stained for insulin, glucagon and proliferating cell nuclear antigen (PCNA), respectively, to qualify the distribution of pancreatic beta and alpha cells and the presence of proliferation in beta cells.

*Islet mass.* This was determined by point counting stereology (Weibel 1972) on Gömori's trichrome-stained sections. Each section was counted systematically with a grid of 100 points (final magnification ×320). The numbers of points over endocrine, exocrine and non-exocrine pancreatic tissue were counted. The relative islet volume was calculated by dividing the number of points over the endocrine tissue by the number of points over the total tissue. Islet mass was determined by multiplying the relative volume by the total weight of the pancreas. A minimum of 500 fields per rat was counted. The islet images for documentation were registered by a CCD camera, coupled to an Olympus BX-60 photomicroscope (Olympus, Tokyo, Japan).

*Immunostaining.* Cellular distribution of insulin, glucagon and PCNA was analysed using a standard indirect immunoperoxidase method. After paraffin removal, the sections were rehydrated and blocked against endogenous peroxidase activity with 1% $H_2O_2$. After washing with 0.01 M phosphate-buffered solution (PBS, pH 7.4) the sections were treated with 0.01 M sodium citrate buffer (0.05% Tween 20, pH 6.0) at 98 °C for antigen retrieval. Sections were then incubated for 30 min with PBS (0.05% Tween 20 and 5% of dry skimmed milk) followed by primary antibody incubation for 2 h at room temperature (RT). The antibodies used were rabbit anti-insulin (Santa Cruz Biotechnology, Santa Cruz, CA, USA), goat anti-glucagon (Santa Cruz biotechnology) and rabbit anti-PCNA (Dako Cytomation, Carpinteria, CA, USA) diluted at 1:150, 1:75 and 1:150 in PBS with 2% of dry skimmed milk respectively. After washes in PBS, sections were incubated at RT for 30 min with LSAB (Dako Cytomation) for insulin or PCNA or with specific biotinylated secondary antibody (Dako Cytomation) for glucagon. Sections were then treated with horseradish peroxidase (HRP)-streptavidin solution from LSAB for insulin or AB system (Dako Cytomation) for glucagon during 30 min at RT. The streptavidin–biotin complexes were detected with diaminobenzidine (DAB) solution (0.1% DAB and 0.02% $H_2O_2$ in PBS). Finally, the sections were rapidly stained with Harris' haematoxylin and mounted for microscopic observation.

*Islet and nucleus area, perimeter and roundness-factor.* Pools of 1000 islets, isolated by collagenase digestion of the pancreas according to a previously published protocol (Rafacho *et al.* 2007, 2008), were collected with a Pasteur pipette and immediately immersion-fixed in 4% paraformaldehyde. Three pools of 1000 islets of each group were used to perform the measurement of total islet area and three other pools were used to determine the nucleus area. For total islet area the islets were submitted to Feulgen's DNA method *en bloc* (Mello 1997) and to determine nucleus area the islets were embedded in historesin (Leica, Wetzlar, Germany), sectioned at 3 μm and submitted to Feulgen's DNA method for posterior analysis. At least 500 islets and 300 nuclei for each group were randomly acquired by a CCD camera. The area ($\mu m^2$) and perimeter (μm) values were automatically obtained by the Image-Pro-Plus ® Media, Cybernetics program, coupled to an Olympus BX-60 photomicroscope. For islet measurements, perimeter values were used to calculate the roundness-factor and the following formula was used [$4\pi \cdot \text{area}/(\text{perimeter})^2$]; for those considered to form a perfect circle, the resulting value was ≥1, and for islets that were not perfect circles, the resulting value was <1.

*Beta-cell proliferation.* Average beta-cell proliferation was obtained by counting total islet-cell nuclei stained for insulin and PCNA, using the software cited above. At least 40 islets (4800 ± 233 beta-cell nuclei) per animal were sampled. The beta-cell proliferation was estimated by the percentage of PCNA-positive cells of the total insulin-positive cells (Terauchi *et al.* 2007).

### *Transmission electron microscopy*

Pools of isolated islets from the experimental groups were processed for transmission electron microscopy, as described previously (De Carvalho *et al.* 1994), employing the fixation procedure according to Cotta-Pereira *et al.* (1976). Briefly, isolated islets were fixed in 3% glutaraldehyde/0.25% tannic acid in Millonig's buffer pH 7.3 for 2 h, postfixed in 1% osmium tetroxide, dehydrated in acetone and finally embedded in araldite resin. After the selection of the regions of interest by trimming the material with a glass knife, ultrathin sections (50–75 nm) obtained with a diamond knife were collected and stained by uranyl acetate and lead citrate. Observation and electron micrographs were made with a LEO–Zeiss 906 transmission electron microscope (Eching bei München, Germany).

### *Insulin content and secretion*

Insulin content and secretion were measured as described in detail previously (Rafacho *et al.* 2007, 2008). Briefly, after

islet isolation, groups of five islets were first incubated for 1 h at 37 °C in a Krebs-bicarbonate buffer solution containing 5.6mmol/l glucose, supplemented with 0.5% of bovine serum albumin and equilibrated with a mixture of 95% $O_2$:5% $CO_2$, pH 7.4. The medium was then replaced by fresh buffer containing 2.8 or 16.7 mmol/l glucose and incubated for a further 1 h. At the end of the incubation, the supernatant was collected and appropriately stored at −20 °C for subsequent measurement of insulin content by RIA, as described above.

### *Protein extraction and immunoblotting*

The following antibodies were used: anti-insulin receptor subtrate-2 (IRS-2) (Cell Signaling, Beverly, MA, USA), anti-alpha-tubulin (used as a housekeeping antibody), anti-AKT, anti-phospho-AKT (ser473) (p-AKT) (Santa Cruz Biotechnology), anti-cyclin $D_2$ (Lab Vision, Fremont, CA, USA), anti-retinoblastoma protein (pRb) (BD Bioscience, Mississauga, ON, CA) and anti-PCNA (Dako Cytomation). Pools of islets were homogenized in ice-cold cell lysis buffer (Cell Signaling) using a cell homogenizer (Fisher Scientific, Suwanee, GA, USA) for 10 s at the maximum speed. Protein concentration from total cell lysate was determined by the RCDC method, according to the manufacturer (Bio-Rad, Hercules, CA, USA). Immunoblotting experiments were performed at least six times. Protein obtained from islets (100 μg) was used for each experiment. After blocking at RT for 2 h in Tris buffer salt tween (TBST)/5% dry skimmed milk, membranes containing islet lysates were washed in TBST (3 × 7 min) and incubated overnight with primary antibodies at the dilutions recommended by the manufacturers in TBST/3% dry skimmed milk. After washing in TBST (3 × 10 min), membranes were incubated with the appropriate secondary antibody conjugated with HRP for 90 min in TBST/1% dried skimmed milk at RT. Antibody binding was detected by enhanced SuperSignal® West Pico Chemiluminescent Substrate (Pierce, Rockford, IL, USA), as described by the manufacturer. Blots were scanned (Epson expression 1600) and the densitometry of protein bands was determined by pixels intensity using Scion Image software (Scion Corporation, Frederick, MD, USA).

### *Statistical analysis*

Results are expressed as the mean ± SEM of the indicated number ($n$) of experiments. Statistical comparisons between data from DEX and CTL groups were performed using the unpaired Student's $t$-test. The significance level adopted was $P < 0.05$.

## Results

### *Development of insulin resistance*

Increases in serum insulin levels and GSIS are features of insulin-resistant rodents (Weir *et al.* 2001). Previous works from our group have demonstrated that rats receiving 1.0 mg/kg DEX showed decreased insulin sensitivity, accompanied by a decrease in glucose tolerance. Increases in circulating serum insulin levels and GSIS were also observed in these rats (Rafacho *et al.* 2007, 2008). Herein, we analysed serum insulin, ipITT and GSIS parameters to confirm the presence of insulin resistance. DEX rats showed a marked increase in fed serum insulin values (25.8 ± 4.2 *vs.* 4.3 ± 0.6 ng/ml for DEX and CTL rats respectively; $n = 10$, $P < 0.05$). During ipITT, DEX rats exhibited decreased insulin sensitivity as shown by a significant reduction in the constant glucose disappearance rate that was threefold lower than that of the CTL ($n = 8$, $P < 0.05$). DEX islets showed a 3.4-fold increase in insulin secretion in islets incubated with 16.7mM glucose, compared to CTL islets (3.82 ± 0.22 *vs.* 13.22 ± 1.02% of islet content for CTL and DEX rats, respectively; $n = 12$, $P < 0.05$).

### *Light microscopic findings in pancreatic islets of DEX rats*

Figure 1(a) shows a panoramic view of a histological section of pancreas from CTL rats. No major histological differences of the exocrine tissue were observed in pancreas from DEX-treated rats. However, varying degrees of islet hyperplasia were more often exhibited by the DEX pancreas (Figure 1c,d). Higher numbers of irregular islets, compared with the rounded and oval islets, were observed in DEX, compared with CTL pancreas (Figure 1c,d). The signs of hyperplasia are generally evidenced by coalescence of adjacent islets (Figure 1c) and enlargement and increased cellularity (Figure 1d). Although mitosis figures are a scarce phenomenon, they were more frequent in DEX, compared with CTL islets (compare Figure 1b with Figure 1e–g).

In CTL rats, beta-cells represent almost all the cells in the islets. The insulin-positive cells occupied the core and mantle of the islet (Figure 2a). Glucagon-positive cells were limited to the ring surrounding the islet (Figure 2b). The pattern of insulin-positive cell distribution in DEX islets was similar to that of CTL islets (Figure 2c). However, there was an apparent discontinuous ring of glucagon-positive cells in DEX islets compared with CTL islets (Figure 2d).

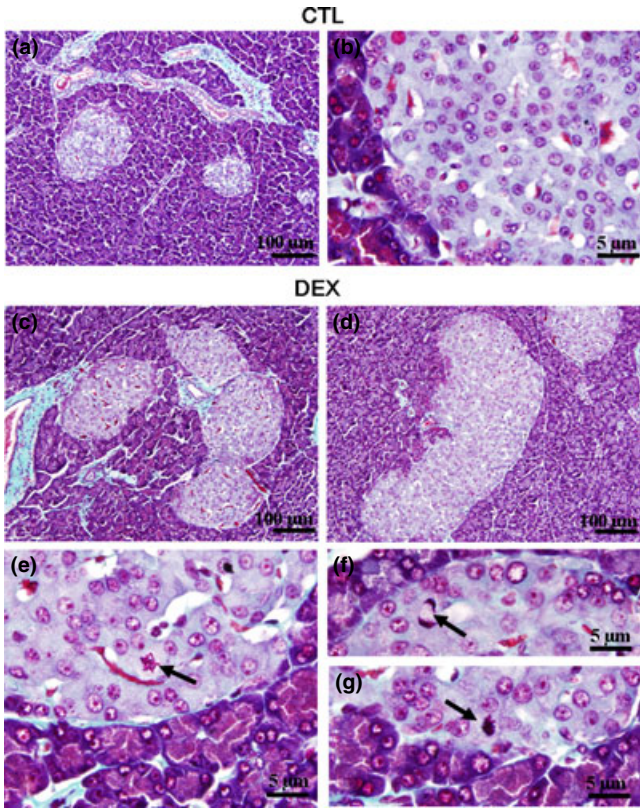


**Figure 1** Morphological aspects of pancreatic islets from DEX and CTL rats. Islets of CTL (a, b) and DEX (c, d) rats. Arrows point to mitotic figures in DEX pancreas (e, g). Light microscope with Gömori's trichrome staining. Magnification ×200 in (a), (c) and (d) and ×1000 in (b), (e), (f) and (g).

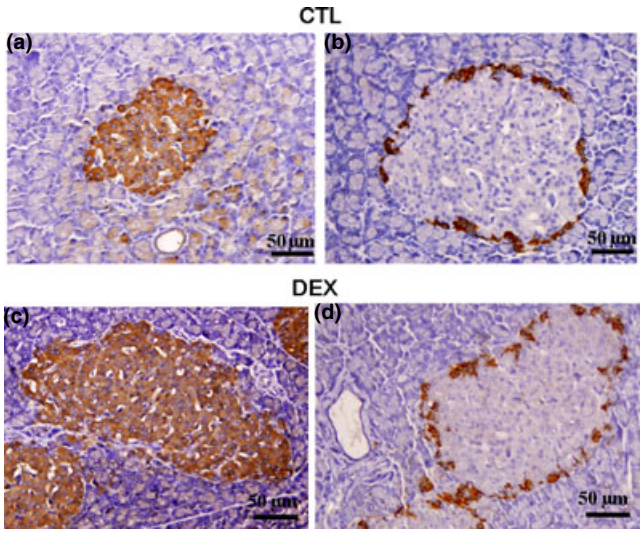


**Figure 2** Cellular distribution of insulin- and glucagon-positive cells in pancreatic islets of DEX and CTL rats. CTL and DEX pancreas immunostained for insulin (a, c) and glucagon (b, d) respectively. Light microscope. Magnification ×400.

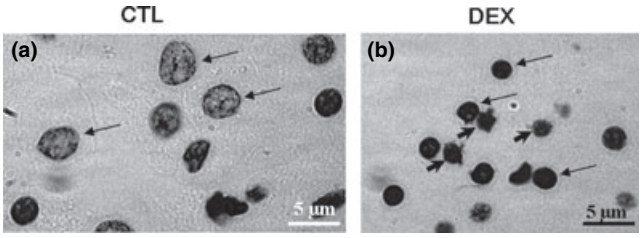


**Figure 3** Nucleus of isolated islets stained by Feulgen's DNA method. Nuclei from CTL (a – arrows) and DEX (b – arrows) islet cells. Occasionally, pyknosis signals and bleb formation indicate the presence of suspect apoptotic phenotypes in DEX islet cells (b – arrowheads). See text for details of morphometrical data. Magnification ×1000.

### *Structural aspects of islet nuclei in DEX rats*

Using Feulgen's DNA method, we observed a well-distributed uniform chromatin, characteristic of normal nuclei, in CTL islet cells (Figure 3a). However, some nuclei from DEX islet cells exhibited a more condensed chromatin compared with CTL islets (Figure 3b). Occasionally, pyknosis signals and bleb formation were observed in DEX-islet cells, indicating the presence of suspect apoptotic phenotypes (arrowheads in Figure 3b). The mean nuclei area and perimeter values were significantly lower in DEX, compared with those observed in CTL islet cells ($n$ = 300, $P < 0.05$; Table 1). DEX islet cell nuclei demonstrated 32% and 20% reductions in area and perimeter values, respectively, compared with CTL.

### *Transmission electron microscopy assays*

Ultrastructural evaluation of isolated DEX and CTL islets confirmed light microscopy results. Pancreatic CTL islet cells (alpha and beta) were easily identified by their characteristic secretory granules (Figure 4b). The secretory granules from pancreatic beta cells featured an electron-dense core and a translucent halo appearance (Figure 4d,e). In DEX islets, alpha and beta cells were also easily distinguishable (Figure 4g). However, DEX beta cells showed an increase in the number of secreting organelles, such as endoplasmic reticulum and Golgi apparatus. The endoplasmic reticulum was preferentially located at the cytoplasm periphery (Figure 4i,k) and the Golgi apparatus at the para-nuclear region (Figure 4h). Mitosis figures were confirmed at the ultrastructural level in DEX beta cells (Figure 4j).

**Table 1** Area and perimeter values from control (CTL) and dexamethasone-treated (DEX) rat islets

| | Area (μm2) | | Perimeter (μm) | | Roundness-factor | |
|---|---|---|---|---|---|---|
| | Islet | Nucleus | Islet | Nucleus | Islet | Nucleus |
| CTL | 12,153 ± 420 | 30.5 ± 0.6 | 432 ± 7 | 21.5 ± 0.2 | 0.75 ± 0.008 | 0.83 ± 0.01 |
| DEX | 26,057 ± 915* | 20.5 ± 0.5* | 672 ± 15* | 17.2 ± 0.2* | 0.69 ± 0.008* | 0.86 ± 0.06* |

Values are mean ± SEM.
*Significantly different *vs.* CTL. $n = 500$ for islet and 300 for nucleus. $P < 0.05$. Unpaired Student's *t*-test.

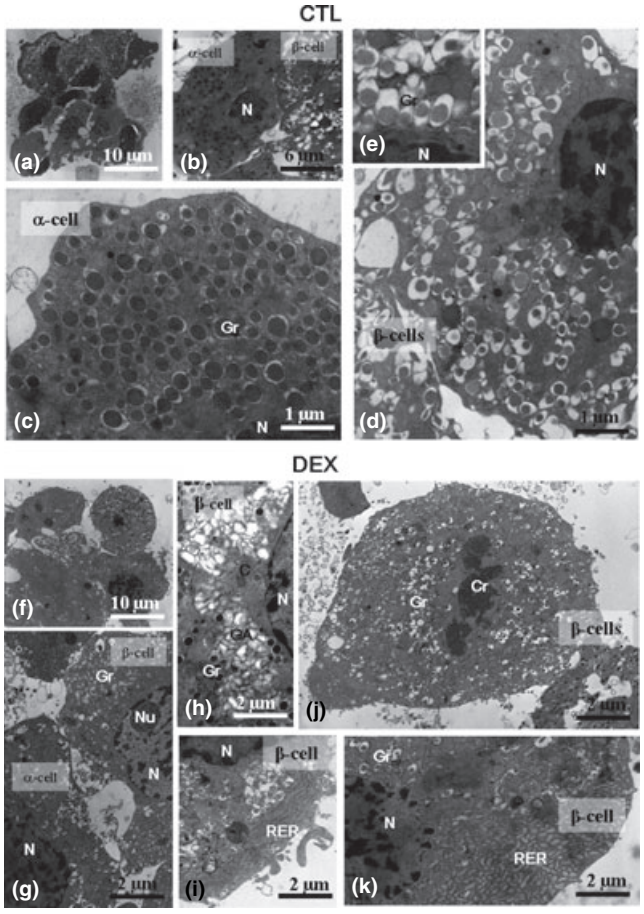


**Figure 4** Transmission Electron Microscopy of isolated islets. General view of the islets (a, f); partial view of the cytoplasm of the alpha and beta cells showing the characteristic granules in CTL and DEX group (b, g, respectively); detailed view of the alpha-cell cytoplasm (c) and of the beta-cell cytoplasm in the CTL group (d) with details of granules (*inset*). Note the increase in the secreting organelles, such as the Golgi apparatus, in the beta-cell cytoplasm (h) and rough endoplasmic reticulum in the peripheral region (i, k) in DEX islet. Mitosis (initial telophasis) figure in the beta cell of DEX islet (j). N, nucleus; Gr, granules; C, centrioles; Cr, chromosomes; Nu, nucleolus; GA, Golgi apparatus; RER, rough endoplasmic reticulum.

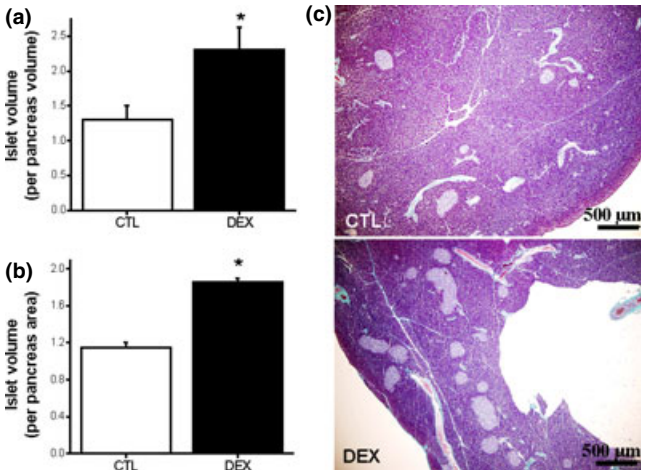


**Figure 5** Increased pancreatic islet mass in insulin-resistant rats. Observe the significant increase in islet volume (a) and islet density (b) in DEX pancreas. Representative image of Gömori's trichrome-stained pancreas section from CTL and DEX groups (c). Data are mean ± SEM. *Significantly different *vs.* CTL. $P < 0.05$; $n = 5$. Unpaired Student's *t*-test. Magnification ×40.

### *Increased pancreatic islet area and mass in pancreas from DEX-treated rats*

Morphometrical parameters indicate marked differences between DEX and CTL islets (Table 1). DEX treatment induced a significant increase in area and perimeter of the islets, compared with CTL islets ($n = 500$, $P < 0.05$). In addition, the roundness-factor value decreased in DEX islets ($n = 500$, $P < 0.05$). The increase in area and perimeter values was 2.1- and 1.5-fold, respectively, in DEX compared with CTL islets (Table 1). The pancreatic islet mass was 1.7-fold higher in DEX, compared with CTL pancreas ($n = 5$, $P < 0.05$; Figure 5a,c). Furthermore, the density of the islets was significantly higher in DEX compared with the CTL group ($n = 5$, $P < 0.05$; Figure 5b,c).

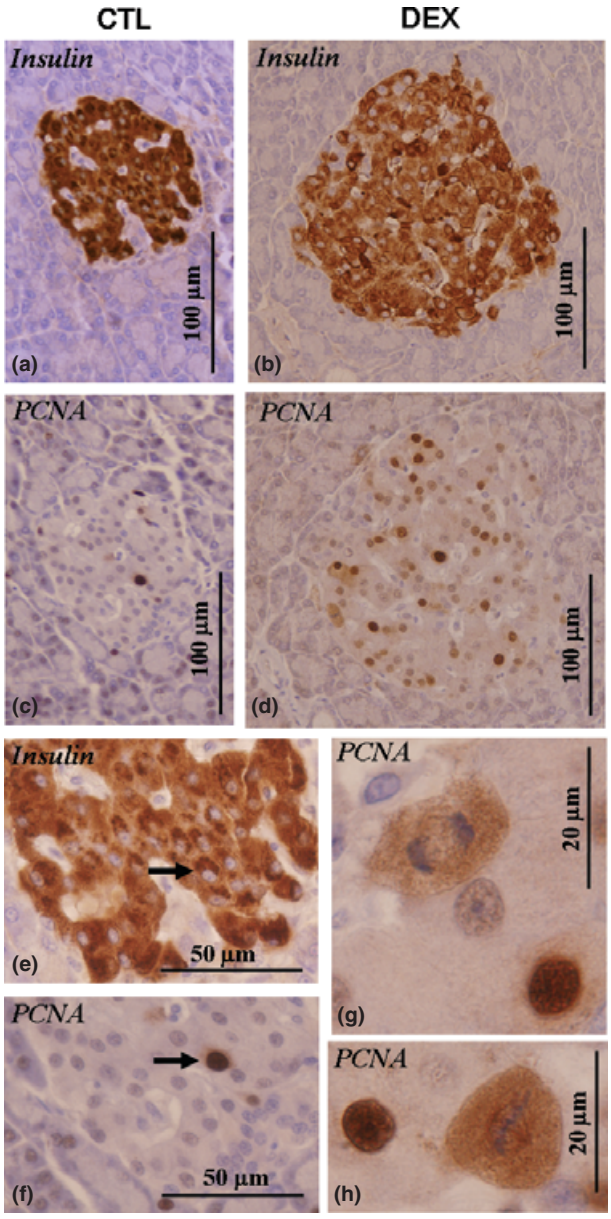


**Figure 6** Light microscopy evaluation of *in situ* anti-PCNA expression in the isolated pancreatic islets. The majority of PCNA-positive cells were related to the beta cell (arrows). Two serial sections were made and one was submitted to anti-PCNA reaction (c, d) and the subsequent section was submitted to anti-insulin reaction (a, b). The increase in PCNA-proliferating cells was notable in DEX islets, including mitotic PCNA-positive figures (d, g, h).

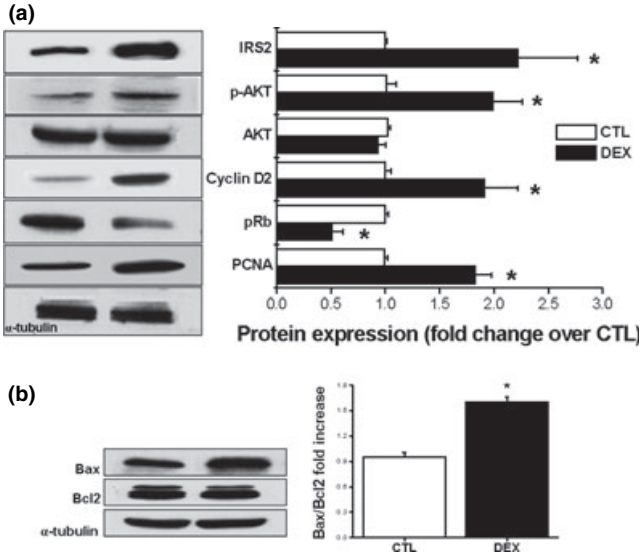


**Figure 7** Increased expression of proteins related to the beta cell proliferation in insulin-resistant rats. Equal amounts of total protein were run in SDS-PAGE from CTL and DEX islets and detected with anti-IRS2, phosphorylated AKT, cyclin $D_2$, pRb and PCNA (a) antibodies. In (b) Bax/Bcl2 protein ratio. Data are mean ± SEM *Significantly different *vs.* CTL. $P < 0.05$; $n = 6$. Unpaired Student's *t*-test.

### *Immunohistochemistry of PCNA and quantification of beta-cell proliferation*

The potential capacity of beta cells for proliferation in both CTL and DEX islets was evaluated at the immunohistochemical level. The PCNA-positive cell was observed in low frequency in pancreatic islets from CTL rats (Figure 6c). Serial section of pancreas stained for insulin confirms the co-localization of PCNA-positive nucleus with beta cell (Figure 6e,f). However, pancreatic beta cells in DEX islets exhibited marked increase in PCNA-positive nuclei (Figure 6d). Figure 6(g,h) shows two PCNA-positive beta cells undergoing mitosis in DEX islets. The quantitative determination of beta-cell proliferation by morphometric analysis revealed a significant increase in beta-cell proliferation in DEX islets ($n = 4$, 800 nuclei; $P < 0.05$). The percentage of PCNA-positive nuclei from total beta cells counted was (15.2 ± 1.2 *vs.* 2.37 ± 0.46% for DEX and CTL, respectively) (compare Figure 6c with Figure 6a and Figure 6d with Figure 6b).

### *Immunoblotting of islets for IRS-2, p-AKT, cyclin $D_2$, pRb, PCNA, Bax and Bcl-2 proteins*

To determine whether the changes in pancreatic beta-cell proliferation in DEX islets were associated with alterations in proteins involved in this event, we performed immunoblotting for IRS-2, p-AKT, AKT, cyclin $D_2$, pRb and PCNA proteins. A 2.2-fold increase in IRS-2 protein expression was observed in DEX islets ($n = 6$, $P < 0.05$; Figure 7a). The phosphorylation levels (but not total protein content) of

 

AKT was also significantly increased in DEX compared with CTL islets ($n = 6$, $P < 0.05$; Figure 7a). Cyclin $D_2$ protein expression exhibited a 1.9-fold increase in DEX islets ($n = 6$, $P < 0.05$; Figure 7a), whereas the expression of total pRb was 0.5-fold decreased in DEX islets ($n = 6$, $P < 0.05$; Figure 7a). In addition, the expression of PCNA was markedly increased (1.8-fold) in DEX compared with CTL islets ($n = 6$, $P < 0.05$; Figure 7a). The ratio between pro-apoptotic Bax and anti-apoptotic Bcl2 proteins increased 1.6-fold in DEX islets ($n = 6$, $P < 0.05$; Figure 7b).

## Discussion

Glucocorticoid-induced insulin resistance is a useful model for the study of the pathogenesis of insulin resistance. Recently, we demonstrated that short-term administration of different concentrations of DEX resulted in a varied degree of insulin resistance without overt installation of type 2 diabetes (Rafacho *et al.* 2008). The insulin-resistant rats used in the present study showed endocrine pancreas adaptations, as judged by the increase in islet function, mass and beta-cell proliferation. We showed, for the first time, in DEX-induced insulin resistance, that the potential mechanisms underlying these events are activation of the IRS-2/AKT pathway and cell cycle activation with the participation of cyclin $D_2$.

To compensate for insulin resistance, the endocrine pancreas undergoes morphological and functional alterations. We, herein, show that DEX rats exhibit hyperinsulinaemia and increased GSIS, supporting the functional improvement of islets in this condition. The increase in plasma insulin levels and the response to glucose of islets from glucocorticoid-treated rodents have been previously described by others (Ogawa *et al.* 1992; Barbera *et al.* 2001; Novelli *et al.* 1999; Rafacho *et al.* 2007).

Studies on the structure of pancreatic islets during insulin resistance induced by glucocorticoids have already been documented (Boquist 1972; Visser *et al.* 1979; Jonas *et al.* 1983; Tomita *et al.* 1984; Zwicker & Eyster 1993; Rafacho *et al.* 2007). The morphological alterations described by these authors included hypertrophy and hyperplasia of islets and beta cells, increase in islet vascularization and occasional mitotic figures. No alterations are observed with regard to the distribution of exocrine and endocrine cells. These results correlate well with hyperinsulinaemia (Boquist 1972; Visser *et al.* 1979; Tomita *et al.* 1984; Rafacho *et al.* 2007). Here, we have also observed several hypertrophic DEX islets with a reduction in roundness-factor and signs of hyperplasia of varied degrees. Increased vascularization was also observed (data not shown); furthermore, the normal distribution of insulin-positive cells within the islets agrees with previous studies in hypertrophic islets (Spencer *et al.* 1986; Zwicker & Eyster 1993). However, glucagon-positive cells exhibited an apparent discontinued ring in DEX islets. In accordance with this observation, islets from KKAy mice show a reduction in alpha-cell area and these cells projected from the periphery to the centre; this projection was often sparse (Diani *et al.* 1987). Nevertheless, the absolute number of alpha cells is not altered in these mice islets; instead, the relative area reduction reflects the increased absolute beta-cell number, which is in agreement with our results for beta-cell proliferation in DEX islets.

Ultrastructural studies of islets during endocrine pancreatic dysfunction are scarce (Jonas *et al.* 1983; Janssen *et al.* 2003; Momose *et al.* 2006). These studies show modifications in the relative amount and aspect of some organelles, including secretory granules. In the present study, we observed an increase in secreting organelles, such as endoplasmic reticulum and Golgi apparatus in DEX islets, indicating hyperfunction. Similar alterations in secreting organelles occur in a diabetic model, the 21-week-old GK mice, at a few weeks before the development of overt diabetes. The beta cells of these mice present cytoplasm occupied with large amounts of enlarged small-sized endoplasmic reticulum with a reduction in the number of insulin granules (Momose *et al.* 2006).

The relative and absolute endocrine cell area or volume, especially of the beta cell, can be modified by experimental and pathophysiological conditions (Tomita *et al.* 1984; Zwicker & Eyster 1993; Gómez Dumm *et al.* 1995; Janssen *et al.* 2001). Morphometric analysis of some quantitative parameters was then performed to evaluate possible changes during the onset of insulin resistance. An increase in islet area and perimeter, as well as in the absolute mass and relative density, of the islets in DEX pancreas was observed. These results are in accordance with previous observations and indicate an adaptive mechanism to compensate for peripheral insulin action impairment imposed by DEX (Tomita *et al.* 1984; Ogawa *et al.* 1992; Rafacho *et al.* 2007). Another revealing result obtained in this study is the marked increase in PCNA staining in beta cells from DEX islets. DEX islets exhibited an increase of more than sixfold in beta-cell proliferation. PCNA is an indicator for cell proliferation and has been used to determine beta-cell mass expansion (Zhang *et al.* 2005; Lipsett *et al.* 2006; Terauchi *et al.* 2007; Vasavada *et al.* 2007). The marked increase in the ratio of beta-cell proliferation in DEX islets was not accompanied by a similar increase in islet mass. The maintenance of beta-cell mass is a dynamic process resulting from a balance between neogenesis, proliferation, cell volume changes

and cell death (Bonner-Weir 2000, 2001). It was demonstrated recently that the absolute increase in beta-cell proliferation might not reflect an increase in beta-cell mass in a glucose-infused mouse model (Alonso *et al.* 2007). Herein, the 6.4-fold increase in beta-cell proliferation includes all cells that have been through S phase during the 5-day administration of DEX. However, we observed an increase in Bax/Bcl2 protein ratio indicating a positive trend for activation of cell death in DEX rats. Thus, these data could explain, in part, the moderate increase in absolute islet mass in DEX rats.

Literature reporting the control of cell cycle events in beta cells is recent, in part, because of a long-standing belief that beta cells cannot replicate. Several groups have tried to elucidate the control of the beta-cell mass (see a list of works in recent reviews: Heit *et al.* 2006; Vasavada *et al.* 2006). Herein, we found a marked increase in islet mass and beta-cell proliferation, accompanied by an increase in IRS-2 and p-AKT levels in insulin-resistant animals. Several approaches, *in vivo* or *in vitro*, with pancreatic beta cells have confirmed the participation of growth factors in the modulation of beta-cell proliferation and expansion (Villanueva-Peñacarrillo *et al.* 1999; Garcia-Ocaña *et al.* 2000; Amaral *et al.* 2004; Friedrichsen *et al.* 2006; Okada *et al.* 2007). Between the several pathways most known to mediate beta-cell proliferation is the IRS-2/PI3K/AKT/p70S6K cascade (Lingohr *et al.* 2002; Okada *et al.* 2007). We believe that high circulating insulin, rather than mild glucose levels, exerts a positive and autocrine effect on beta-cell proliferation via insulin signalling in DEX-treated rats.

Consistent with this result, insulin infusion stimulates beta-cell proliferation and increases beta-cell mass in rats (Paris *et al.* 2003). Moreover, a recent study showed that insulin, but not IGF-1, is crucial to the glucose-stimulated beta-cell proliferation. Incubating MIN6 cells with high glucose in the presence of an anti-insulin antibody almost abolished the rate of proliferation (Muller *et al.* 2006). Studies in mice lacking IRS-2 further support the role of insulin in beta-cell replication (Withers *et al.* 1998; Kushner *et al.* 2002). Taken together, these data implicate the IR/IRS-2/PI3K/AKT pathway as a mediator of beta-cell proliferation in insulin-resistant rats.

The increase in cyclin $D_2$ and decrease in pRb protein content were also observed in DEX islets. Activation of AKT in pancreatic beta cells resulted in a marked expansion of beta-cell mass, due to an increase in beta-cell proliferation and size, which is associated with increased cyclin $D_1$, cyclin $D_2$, and p21 levels and CDK4 activity (Fatrai *et al.* 2006). Thus, in DEX rats, the increased levels of phosphorylated AKT might maintain, at least partially, the higher levels of cyclin $D_2$ protein. Recently, pRb loss in pancreatic islets was observed not to result in increased islet volume, density and beta-cell proliferation (Vasavada *et al.* 2007). Although pRb seems not to be essential in the transgenic mice model, we cannot rule out the possible participation of diminished pRb protein content, favouring the release of cell cycle progression in our DEX rats. Finally, we did not address whether the alterations in the protein contents are mediated by a direct effect of DEX. However, two lines of evidence favour the idea that this alteration is the result of indirect insulin resistance rather than a direct effect of DEX treatment. First, DEX incubation of airway smooth muscle cells induced cell proliferation inhibition, concomitant with decreased cyclin $D_1$ protein expression and decreased phosphorylation of pRb protein. Secondly, in transgenic mice models ($IR^{+/-}$, IRS-$1^{-/-}$, $IR^{+/-}$/IRS-$1^{+/-}$) that exhibit insulin resistance and hyperinsulinaemia, the IRS-2 pathway drives beta-cell hyperplasia (Araki *et al.* 1994; Tamemoto *et al.* 1994; Bruning *et al.* 1997; Kido *et al.* 2000). Zucker fatty rats (Pick *et al.* 1998) also present hyperinsulinaemia, mild blood glucose levels and beta-cell hyperplasia like DEX rats. Based on these data, we are tempted to believe that the proteins altered herein (IRS-2, AKT and cyclin D2), which are potential mediators of beta-cell hyperplasia, are positively regulated by circulating insulin.

In summary, we have generated an insulin-resistant animal by short-term administration of DEX. Under these conditions, compensations by the beta cell are observed, including increases in islet function, islet mass and beta-cell proliferation. The potential mechanisms that underlie these events are the activation of the IRS-2/AKT pathway and cell cycle activation, mediated by cyclin $D_2$.

## Acknowledgements

This study is part of the doctoral thesis of A.R. and was supported by grants from the Brazilian foundations FAPESP and CNPQ. S.R.T. expresses his gratitude to The Brazilian National Research and Development Council (CNPq – proc. no. 3011111/2005-7 research fellowship). The authors are indebted to Luiz Roberto Falleiros Jr for technical assistance and to Nicola Conran for editing the English.

## References

Alonso L.C., Yokoe T., Zhang P. *et al.* (2007) Glucose infusion in mice. A new model to induce β-cell replication. *Diabetes* **56**, 1792–1801.

Amaral M.E., Cunha D.A., Anhê G.F. *et al.* (2004) Participation of prolactin receptors and phosphatidylinositol 3-kinase and MAP kinase pathways in the increase in pancreatic islet mass and sensitivity to glucose during pregnancy. *J. Endocrinol.* **183**, 469–476.

Anderson J.W., Kendall C.W., Jenkins D.J. (2003) Importance of weight management in type 2 diabetes: review with meta-analysis of clinical studies. *J. Am. Coll. Nutr.* **22**, 331–339.

Araki E., Lipes M.A., Patti M.E. *et al.* (1994) Alternative pathway of insulin signalling in mice with targeted disruption of the IRS-1 gene. *Nature* **372**, 186–190.

Barbera M., Fierabracci V., Novelli M. *et al.* (2001) Dexamethasone-induced insulin resistance and pancreatic adaptive response in aging rats are not modified by oral vanadyl sulfate treatment. *Eur. J. Endocrinol.* **145**, 799–806.

Beard J.C., Halter J.B., Best J.D., Pfeifer M.A., Porte D. Jr (1984) Dexamethasone-induced insulin resistance enhances B cell responsiveness to glucose level in normal men. *Am. J. Physiol.* **247**, E592–E596.

Bonner-Weir S. (2000) Life and death of the pancreatic beta cells. *Trends Endocrinol. Metab.* **11**, 375–378.

Bonner-Weir S. (2001) Beta-cell turnover: its assessment and implications. *Diabetes* **50**, S20–S24.

Bonner-Weir S., Trent D.F., Zmachinski C.J., Clore E.T., Weir G.C. (1981) Limited B cell regeneration in a B cell deficient rat model: studies with dexamethasone. *Metabolism* **9**, 914–918.

Boquist L. (1972) Obesity and pancreatic islet hyperplasia in the Mongolian gerbil. *Diabetologia* **8**, 274–282.

Bruning J.C., Winnay J., Bonner-Weir S., Taylor S.I., Accili D., Kahn C.R. (1997) Development of a novel polygenic model of NIDDM in mice heterozygous for IR and IRS-1 null alleles. *Cell* **88**, 561–572.

Burén J., Liu H.X., Jensen J., Eriksson J.W. (2002) Dexamethasone impairs insulin signaling and glucose transport by depletion of insulin receptor substrate-1, phosphatidylinositol 3-kinase and protein kinase B in primary cultured rat adipocytes. *Eur. J. Endocrinol.* **146**, 419–429.

Cotta-Pereira G., Rodrigo F.G., David-Ferreira J.F. (1976) The use of tannic acid-glutaraldehyde in the study of elastic related fibers. *Stain Technol.* **51**, 7–11.

Cozar-Castellano I., Takane K.K., Bottino R., Balamurugan A.N., Stewart A.F. (2004) Induction of beta-cell proliferation and retinoblastoma protein phosphorylation in rat and in human islet using adenovirus-mediated transfer of cyclin-dependent kinase-4 and cyclin $D_1$. *Diabetes* **53**, 149–159.

De Carvalho H.F., Lino Neto J., Taboga S.R. (1994) Microfibrils: neglected components of pressure-bearing tendons. *Ann. Anat.* **176**, 155–159.

Diani A.R., Sawada G.A., Hannah B.A. *et al.* (1987) Analysis of pancreatic islet cells and hormone content in the spontaneously diabetic KKAy mouse by morphometry, immunocytochemistry and radioimmunoassay. *Virch. Arch. A. Pathol. Anat. Histopathol.* **412**, 53–61.

Fatrai S., Elghazi L., Balcazar N. *et al.* (2006) AKT induces beta-cell proliferation by regulating cyclin D1, cyclin D2, and p21 levels and cyclin-dependent kinase-4 activity. *Diabetes* **55**, 318–325.

Fernández E., Angeles Mártin M., Fajardo S., Escrivá F., Álvarez C. (2006) Increased IRS-2 content and activation of IGF-1 pathway contribute to enhance B-cell mass in fetuses from undernourished pregnant rats. *Am. J. Physiol. Endocrinol. Metab.* **292**, E187–E195.

Friedrichsen B.N., Neubauer N., Lee Y.C. *et al.* (2006) Stimulation of pancreatic β-cell replication by incretins involves transcriptional induction of cyclin D1 via multiple signalling pathways. *J. Endocrinol.* **188**, 481–492.

Garcia-Ocaña A., Takane K., Syed M.A., Phlibrick W.M., Vasavada R.C., Stewart A.F. (2000) Hepatocyte growth factor overexpression in the islet of transgenic mice increases beta cell proliferation, enhances islet mass and induces mild hypoglycemia. *J. Biol. Chem.* **275**, 1226–1232.

Gómez Dumm C.L.A., Cónsole M., Luna G.C., Dardene M., Goya R.G. (1995) Quantitative immunohistochemical changes in the endocrine pancreas of nonobese diabetic (NOD) mice. *Pancreas* **11**, 396–401.

Heit J.J., Karnik S.K., Kim S.K. (2006) Intrinsic regulators of pancreatic β-cell proliferation. *Ann. Rev. Cell. Dev. Biol.* **22**, 311–338.

Holness M.J., Smith N.D., Greenwood G.K., Sugden M.C. (2005) Interactive influences of peroxisome proliferator-activated receptor α activation and glucocorticoids on pancreatic beta cell compensation in insulin resistance induced by dietary saturated fat in the rat. *Diabetologia* **48**, 2062–2068.

Hoogwerf B. & Danese R.D. (1999) Drug selection and the management of corticosteroid-related diabetes mellitus. *Rheum. Dis. Clin. North Am.* **25**, 489–505.

Janssen S.W., Hermus A.R., Lange W.P. *et al.* (2001) Progressive histopathological changes in the pancreatic islets during aging of Zucker diabetic fatty rats. *Exp. Clin. Endocrinol. Diabetes* **109**, 273–282.

Janssen S.W., Martens G.J., Sweep C.G., Span P.N., Verhofstad A.A., Hermus A.R. (2003) Phlorizin treatment prevents the decrease in plasma insulin levels but not the progressive histopathological changes in the pancreatic islets during age of Zucker diabetic fatty rats. *J. Endocrinol. Invest.* **26**, 508–515.

Jonas L., Putzke H.P., Hahn von Dorsche H. (1983) Islands of Langerhans of rats (*Rattus norvegicus*, Forma alba) after high prednisolone dosage – a semiquantitative light and electron microscopic study. *Anat. Anz.* **154**, 273–282.

Kido Y., Burks D.J., Withers D. *et al.* (2000) Tissue-specific insulin resistance in mice with mutations in the insulin receptor, IRS-1, and IRS-2. *J. Clin. Invest.* **105**, 199–205.

 

Kushner J.A., Ye J., Schubert M. *et al.* (2002) Pdx1 restores β cell function in Irs2 knockout mice. *J. Clin. Invest.* **109**, 1193–1201.

Lingohr M.K., Dickson L.M., McCuaig J.F., Hugl S.R., Twardzik D.R., Rhodes C.J. (2002) Activation of IRS-2-mediated signal transduction by IGF-1, but not TGF-alpha or EGF, augments pancreatic beta-cell proliferation. *Diabetes* **51**, 966–976.

Lipsett M.A., Austin E.B., Castellarin M.L., Lemay J., Rosenberg L. (2006) Evidence for the homeostatic regulation of induced beta cell mass expansion. *Diabetologia* **49**, 2910–2919.

Mello M.L.S. (1997) Cytochemistry of DNA, RNA and nuclear proteins. *Braz. J. Genet.* **20**, 257–264.

Momose K., Nunomiya S., Nakata M., Yada T., Kikuchi M., Yashiro T. (2006) Immunohistochemical and electron-microscopic observation of B-cells in pancreatic islets of spontaneously diabetic Goto-Kakizaki rats. *Med. Mol. Morphol.* **39**, 146–153.

Muller D., Jones P.M., Persaud S.J. (2006) Autocrine anti-apoptotic and proliferative effects of insulin in pancreatic b-cells. *FEBS Lett.* **580**, 6977–6980.

Nicod N., Giusti V., Besse C., Tappy L. (2003) Metabolic adaptations to dexamethasone-induced insulin resistance in healthy volunteers. *Obes. Res.* **11**, 625–631.

Niessen A. (2006) On the role of IRS2 in the regulation of functional ß-cell mass. *Arch. Physiol. Biochem.* **112**, 65–73.

Novelli M., De Tata V., Bombara M. *et al.* (1999) Insufficient adaptive capability of pancreatic endocrine function in dexamethasone-treated ageing rats. *J. Endocrinol.* **162**, 425–432.

Ogawa A., Johnson J.H., Ohneda M. *et al.* (1992) Roles of insulin resistance and ß-cell dysfunction in dexamethasone-induced diabetes. *J. Clin. Invest.* **90**, 497–504.

Okada T., Liew C.W., Hu J. *et al.* (2007) Insulin receptors in β-cells are critical for islet compensatory growth response to insulin resistance. *Proc. Natl Acad. Sci. USA* **104**, 8977–8982.

Pagano G., Cavallo-Perin P., Cassader M. *et al.* (1983) An in vivo and in vitro study of the mechanism of prednisone-induced insulin resistance in healthy subjects. *J. Clin. Invest.* **72**, 1814–1820.

Paris M., Bernard-Kargar C., Berthault M.F., Bouwens L., Ktorza A. (2003) Specific and combined effects of insulin and glucose on functional pancreatic β-cell mass in vivo in adult rats. *Endocrinology* **144**, 2717–2727.

Pick A., Clark J., Kubstrup C. *et al.* (1998) Role of apoptosis in failure of beta-cell mass compensation for insulin resistance and beta-cell defects in the male Zucker diabetic fatty rat. *Diabetes* **47**, 358–364.

Rafacho A., Roma L.P., Taboga S.R., Boschero A.C., Bosqueiro J.R. (2007) Dexamethasone-induced insulin resistance is associated with increased connexins 36 mRNA and protein expression in pancreatic rat islets. *Can. J. Physiol. Pharmacol.* **53**, 881–885.

Rafacho A., Giozzet V.A.G., Boschero A.C., Bosqueiro J.R. (2008) Functional alterations in endocrine pancreas of rats with different degrees of dexamethasone-induced insulin resistance. *Pancreas* **36**, 284–293.

Ruzzin J., Wagman A.S., Jensen J. (2005) Glucocorticoid-induced insulin resistance in skeletal muscles: defects in insulin signaling and the effects of a selective glycogen synthase kinase-3 inhibitor. *Diabetologia* **48**, 2119–2130.

Saad M.J., Folli F., Kahn J.A., Kahn C.R. (1993) Modulation of insulin receptor, insulin receptor substrate-1, and phosphatidylinositol 3-kinase in liver and muscle of dexamethasone-treated rats. *J. Clin. Invest.* **92**, 2065–2072.

Scott A.M., Atwater I., Rojas E. (1981) A method for the simultaneous measurement of insulin release and B cell membrane potential in single mouse islets of Langerhans. *Diabetologia* **21**, 470–475.

Severino C., Brizzi P., Solinas A., Secchi G., Maioli M., Tonolo G. (2002) Low-dose dexamethasone in the rat. A model to study insulin resistance. *Am. J. Physiol.* **283**, E367–E373.

Spencer A.J., Andreu M., Greaves P. (1986) Neoplasia and hyperplasia of pancreatic endocrine tissue in the rat: an immunocytochemical study. *Vet. Pathol.* **23**, 11–15.

Tamemoto H., Kadowaki T., Tobe K. *et al.* (1994) Insulin resistance and growth retardation in mice lacking insulin receptor substrate-1. *Nature* **372**, 182–186.

Terauchi I., Takamoto I., Kubota N. *et al.* (2007) Glucokinase and IRS-2 are required for compensatory B cell hyperplasia in response to high-fat diet-induced insulin resistance. *J. Clin. Invest.* **117**, 246–257.

Tomita T., Visser P., Friesen S., Doull V. (1984) Cortisone-induced islet cell hyperplasia in hamsters. *Virch. Arch. B Cell Pathol. Incl. Mol. Pathol.* **45**, 85–95.

Vasavada R.C., Gonzáles-Pertusa J.A., Fujinaka I., Fiaschi-Taesch N., Cozar-Castellano I., Garcia-Ocaña A. (2006) Growth factors and beta cell replication. *Int. J. Biochem. Cell Biol.* **38**, 931–950.

Vasavada R.C., Cozar-Castellano I., Sipula D., Stewart A.F. (2007) Tissue-specific deletion of the retinoblastoma protein in the pancreatic B-cell has limited effects on B-cell replication, mass, and function. *Diabetes* **56**, 57–64.

Villanueva-Peñacarrillo M.L., Cancelas J., de Miguel F. *et al.* (1999) Parathyroid hormone-related peptide stimulates DNA synthesis and insulin secretion in pancreatic islets. *J. Endocrinol.* **163**, 403–408.

Visser P.A., Pierce G.E., Tomita T., Friesen S.R. (1979) Stimulation of pancreatic islet hypertrophy and beta-cell hyperplasia in Syrian hamsters. *Surg. Forum* **30**, 310–311.

Weibel E.R. (1972) The value of stereology in analysing structure and function of cells and organs. *J. Microsc.* **95**, 3–13.

Weir G.C., Laybutt D.R., Kaneto H., Bonner-Weir S., Sharma A. (2001) Beta-cell adaptation and decompensation during the progression of diabetes. *Diabetes* **50**, S154–S159.

Withers D.J., Gutierrez J.S., Towery H., Burks D.J., Ren J.M. *et al.* (1998) Disruption of IRS-2 causes type 2 diabetes in mice. *Nature* **391**, 900–904.

Zhang X., Gaspard J.P., Mizukami Y., Li J., Graeme-Cook F., Chung D.C. (2005) Overexpression of cyclin D1 in pancreatic beta-cells in vivo results in islet hyperplasia without hypoglycemia. *Diabetes* **54**, 712–719.

Zwicker G.M. & Eyster R.C. (1993) Chronic effects of corticosteroid oral treatment in rats on blood glucose and serum insulin levels, pancreatic islet morphology, and immunostaining characteristics. *Toxicol. Pathol.* **21**, 502–508.

 